

High-temperature behavior of vanadyl pyrophosphate $(\text{VO})_2\text{P}_2\text{O}_7$

Sander van Smaalen^{a,*}, Robert Dinnebier^b, Jonathan Hanson^c, Jan Gollwitzer^a,
Frank Büllersfeld^d, Andrei Prokofiev^d, Wolf Assmus^d

^aLaboratory of Crystallography, University of Bayreuth, 95440 Bayreuth, Germany

^bMax Planck Institute for Solid State Research, Stuttgart, Germany

^cChemistry Department, Brookhaven National Laboratory, Upton, NY 11973-5000, USA

^dInstitute of Physics, University of Frankfurt, D-60054 Frankfurt am Main, Germany

Received 11 March 2005; received in revised form 29 April 2005; accepted 30 April 2005

Available online 1 June 2005

Abstract

$(\text{VO})_2\text{P}_2\text{O}_7$ has been studied at high temperatures by in situ X-ray powder diffraction in an inert atmosphere. Lattice parameters indicate an anisotropic thermal expansion up to $T_c = 214^\circ\text{C}$, followed by an approximately isotropic expansion up to 490°C . It is proposed that T_c is the temperature of a second-order phase transition between the known room temperature form with space group $Pca2_1$ and a high-temperature form with space group $Pcab$. Above 490°C a minority phase develops in the sample that was identified as the V^{3+} containing compound $\text{V}_4(\text{P}_2\text{O}_7)_3$, while the anisotropic expansion along a suggests that stoichiometric $(\text{VO})_2\text{P}_2\text{O}_7$ transforms into $(\text{VO})_2\text{P}_2\text{O}_{7+x}$ with interstitial oxygen located between the layers. With an onset at 706°C all of the $(\text{VO})_2\text{P}_2\text{O}_7$ transforms into VPO_4 .

© 2005 Elsevier Inc. All rights reserved.

PACS: 61.66.Fn; 65.40.De; 61.50.Ks; 61.50.Nw

Keywords: $(\text{VO})_2\text{P}_2\text{O}_7$; Phase transitions; X-ray powder diffraction; Thermal expansion

1. Introduction

Vanadyl pyrophosphate $(\text{VO})_2\text{P}_2\text{O}_7$ is used as an industrial catalyst for the controlled oxidation of alkanes; in particular, for the synthesis of maleic anhydride from *n*-butane [1,2]. All studies have shown that $(\text{VO})_2\text{P}_2\text{O}_7$ is the major component of the catalysts, but the presence of V^{5+} ions has been proposed to be important for catalytic activity [3,4]. Alternatively, VOPO_4 was suggested to be detrimental to catalytic behavior and the presence of both V^{4+} and V^{3+} was proposed to be required for catalysis [4–6]. Furthermore, it appeared that in active catalysts the P:V ratio can be slightly large than 1, thus providing another parameter influencing the possible formation of other

phases [4]. All studies show tuning of the structural and morphological surface structure to be important for catalytic behavior.

Interest in the low-temperature properties of $(\text{VO})_2\text{P}_2\text{O}_7$ concerns its quasi-one-dimensional magnetic properties [7–10]. This interest motivated accurate determinations of the crystal structure, after initial reports suggested either $Pca2_1$ or $Pcam$ or $P2_1$ space groups [3,11,12]. The crystal structure of $(\text{VO})_2\text{P}_2\text{O}_7$ is now well established as orthorhombic with space group $Pca2_1$ for temperatures between 100 and 300 K [13–15] (Fig. 1). Possible superlattice reflections in the diffraction at low temperatures have never been observed, thus rendering a spin-Peierls mechanism for the magnetic order at low temperatures unlikely.

The importance of $(\text{VO})_2\text{P}_2\text{O}_7$ for catalysis makes knowledge of the behavior of this compound at elevated temperatures desirable. Spectroscopic techniques as well

*Corresponding author. Fax: +49 921 55 3770.

E-mail address: smash@uni-bayreuth.de (S. van Smaalen).

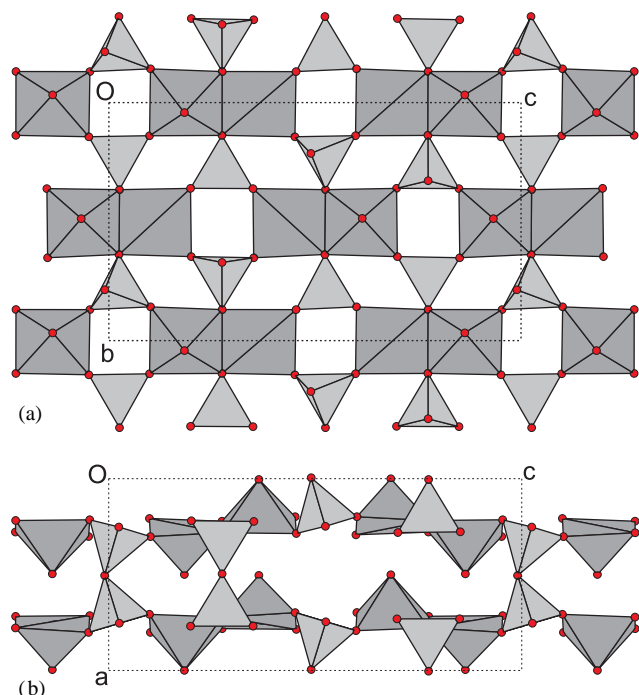


Fig. 1. Crystal structure of $(\text{VO})_2\text{P}_2\text{O}_7$ at 100 K. (a) Projection along c of one layer and (b) projection along b of one double row of PO_4 tetrahedra (light gray) and VO_5 pentagonal prisms (dark gray). Circles indicate oxygen atoms. Coordinates from Ref. [14].

as X-ray powder diffraction have been used for this purpose, but the latter was only applied to quenched samples after high-temperature treatments under different conditions. Here, we report the results of an in situ X-ray powder diffraction study at high temperatures. We have discovered a highly anisotropic thermal expansion that becomes isotropic above 214°C . It is thus suggested that $T_c = 214^\circ\text{C}$ represents a phase transition from the known $Pca2_1$ crystal structure towards a high-temperature form with the centrosymmetric space group $Pcab$. At about 480°C anisotropic expansion sets in again, and at still higher temperatures $(\text{VO})_2\text{P}_2\text{O}_7$ is found to decompose into VPO_4 and a minority phase of $\text{V}_3(\text{P}_2\text{O}_7)_3$.

2. Experimental

$(\text{VO})_2\text{P}_2\text{O}_7$ was prepared by heating $(\text{VO})\text{PO}_4 \cdot \frac{1}{2}\text{H}_2\text{O}$ under argon [12,16]. Single-crystalline material was prepared as described elsewhere [17]. A small piece of single crystal was ground into a fine powder and subsequently loaded into a capillary of diameter 0.3 mm. The capillary was sealed by standard procedures (gas welding), thus leaving a small amount of air above the solid material. This provides an oxygen-free atmosphere after the oxygen has reacted with $(\text{VO})_2\text{P}_2\text{O}_7$ at high temperatures.

In situ X-ray powder diffraction data of $(\text{VO})_2\text{P}_2\text{O}_7$ at high temperatures were collected in transmission with a small environment cell for real-time studies on a motorized goniometer head at beamline X7B at the National Synchrotron Light Source (NSLS) at Brookhaven National Laboratory. As detector, a MAR 345 image plate reader was set up perpendicular to the beam path at a distance of approximately 170 mm from the sample. LaB_6 was used as an external standard to determine the beam center, sample-to-detector distance, exact wavelength ($\lambda = 0.92135 \text{ \AA}$), and tilting angle of the image plate. The sample was contained in a sealed 0.3 mm quartz glass capillary loaded in a 0.8 mm sapphire capillary attached to a flow-reaction cell, similar to those described in [18,19].

The temperature was monitored and controlled by a 0.010 in thermocouple (Omega) which was inserted straight into the sapphire tube adjacent to and contacting the sample capillary. The sample was aligned such that the sample closest to the thermocouple was in the X-ray beam path. The sample was heated in the temperature range from room temperature up to 850°C at $6.58^\circ\text{C}/\text{min}$ with a small resistance heater wrapped around the sapphire tube. During exposure, the samples were rocked for several degrees in order to improve randomization of the crystallites. The exposure time was 80 s plus 80 s for the readout of the image plate. This implies a temperature interval of 17.9348°C between measurements, while each complete diffraction pattern has collected the scattering off the sample over a temperature range of $\Delta T = 8.96^\circ\text{C}$. The total time of the experiment was 125.3 min. Integration of the powder patterns was performed using the program FIT2D [20,21], resulting in diagrams of corrected intensities versus the scattering angle 2θ . Any reflections due to the single-crystal sapphire capillary were excluded. It was observed that the diffracted intensity was quite uniformly distributed over the Debye–Scherrer rings, ruling out severe grain size effects and preferred orientation. Low-angle diffraction peaks had a typical full-width at half-maximum (FWHM) of 0.16° in 2θ . Data reduction on all powder diffraction patterns was performed using the Powder3D program [22].

Visual inspection of the series of diffraction patterns showed that a second phase starts to develop at $T = 491.3^\circ\text{C}$, while $(\text{VO})_2\text{P}_2\text{O}_7$ transforms into a new phase between $T = 706.5$ and 796.2°C (Fig. 2).

LeBail fits showed that the diagrams up to 473.4°C could be indexed by unit cells corresponding to $(\text{VO})_2\text{P}_2\text{O}_7$ (Table 1). The indexing was confirmed by Rietveld refinements, employing the known crystal structure [14,15]. One diffraction maximum at $2\theta \approx 15.6^\circ$ was identified as due to quartz. This peak was observed at all temperatures, and quartz might have contaminated the sample through abrasion of the agate mortar during the prolonged grinding of the sample. A

good fit to the data was obtained by refinement of only the scale factor and an overall temperature factor. This fit was improved upon refinement of the atomic coordinates, but standard uncertainties (s.u.) in the latter amounted up to 0.2 Å. The good fit to the

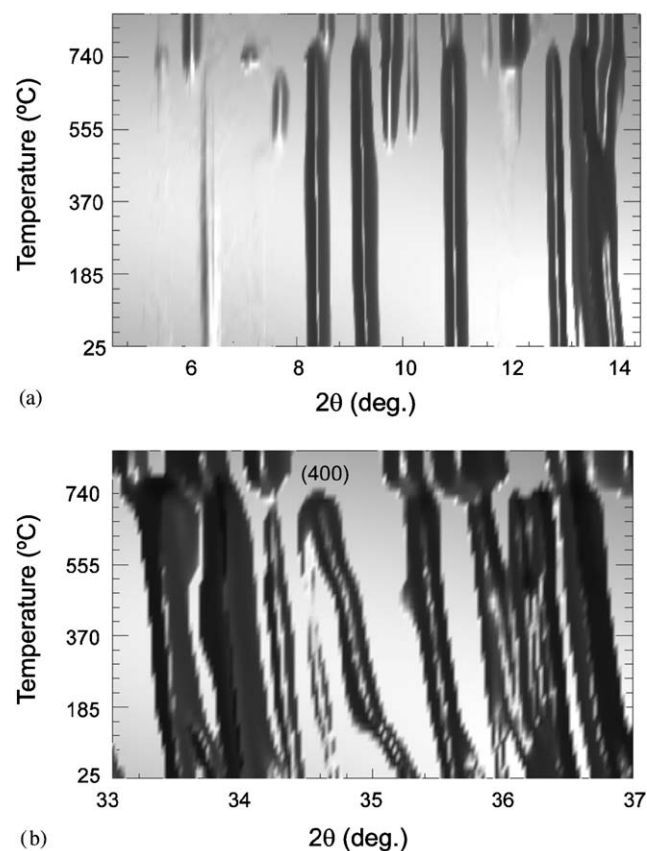


Fig. 2. X-ray diffraction as a function temperature. (a) Diffraction at low angles 2θ . The development of a second phase starting around 500 °C and the phase transformation at about 730 °C are clearly visible and (b) diffraction at high angles 2θ . The (400) reflection shows the thermal expansion of the lattice parameter a . This reflection disappears at the phase transformation. Lowest temperature is 25 °C; highest temperature is 850 °C.

Table 1

R values for the fit to the diffraction data for selected temperatures at which $(\text{VO})_2\text{P}_2\text{O}_7$ is the major phase

Temperature (°C)	LeBail	R_p		R_{obs}	
		$Pca2_1$	$Pcab$	$Pca2_1$	$Pcab$
42.9	0.025	0.033	0.035	0.041	0.047
473.4	0.027	0.038	0.040	0.062	0.068
688.6	0.021	0.033	0.036	0.084	0.095

R_p is the profile R -value and R_{obs} is the Bragg R -value. Results are given for Rietveld refinements in the space groups $Pca2_1$ and $Pcab$ as well as for the LeBail fit.

diffraction data proves that the compound is $(\text{VO})_2\text{P}_2\text{O}_7$ indeed, but the large s.u. on the atomic coordinates show that accurate crystal structures cannot be obtained from the Rietveld refinements. The LeBail fits provided the lattice parameters as a function of temperature and thus gave the thermal expansion (Fig. 3). LeBail fits were performed with the computer program GSAS [23]. Rietveld refinements were performed alternatively with GSAS and JANA2000 [24].

It is noticed, that the structure of $(\text{VO})_2\text{P}_2\text{O}_7$ can approximately be described in the centrosymmetric space group $Pcab$, which was not considered before [11]. In order to map the $Pca2_1$ structure onto $Pcab$, shifts are required of up to 0.06 Å for the V and P atoms and of up to 0.35 Å for the oxygen atoms, showing that the major part of the deviation from $Pcab$ is rotations of the polyhedral groups. The single-crystal data at $T = 100$ K are significantly better fitted in $Pca2_1$ ($R_F = 0.031$) than in $Pcab$ ($R_F = 0.096$), while many

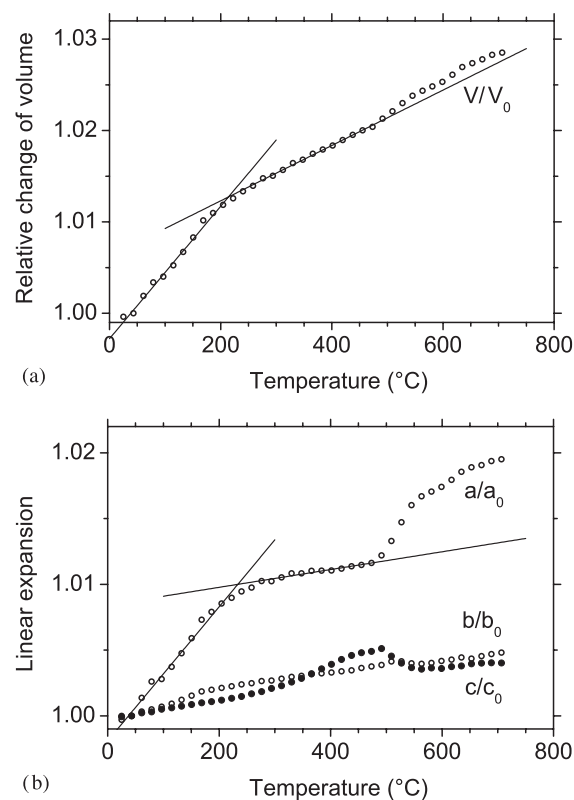


Fig. 3. Thermal expansion of $(\text{VO})_2\text{P}_2\text{O}_7$ as determined by in situ X-ray diffraction. (a) Temperature dependence of the unit cell volume and (b) relative changes of the lattice parameters. Values have been normalized to the values at $T = 42.9$ °C, which are $a_0 = 7.7288(1)$, $b_0 = 9.5787(2)$, $c_0 = 16.5873(2)$ Å and $V_0 = 1228.0$ Å³. Straight lines are the result of linear fits to the points up to 150.5 °C and to the points between 240.2 and 473.4 °C. They give different low-temperature and intermediate temperature expansion coefficients: $\alpha_V^{\text{LT}} = 7.2(4)10^{-5}$; $\alpha_V^{\text{HT}} = 3.03(5)10^{-5}$; $\beta_a^{\text{LT}} = 5.1(3)10^{-5}$; and $\beta_a^{\text{HT}} = 0.68(5)10^{-5}$. The intersection of the two lines in Fig. 3a provides the transition temperature $T_c = 214.1$ °C.

reflections have been observed that violate the *b*-glide [14]. However, the powder diffraction data do not give significant intensities for any of these forbidden reflections, as can be explained by the relatively high background in the data. Although the Rietveld fits in *Pca*2₁ are slightly better than those in *Pcab* at all temperatures, the latter space group has half the number of independent parameters and inspection of the profiles indicate fits to the data of comparable quality (Fig. 4). Therefore, it is concluded that the data are insufficiently accurate to distinguish between *Pca*2₁ and *Pcab* by refinements. However, the thermal expansion shows an anomaly at 214.1 °C, indicating a second-order phase transition to occur at this temperature (Fig. 3a). Together with a good fit of a structure in *Pcab* this strongly suggests that above 214.1 °C (VO)₂P₂O₇ is centrosymmetric *Pcab*. This interpretation is in accor-

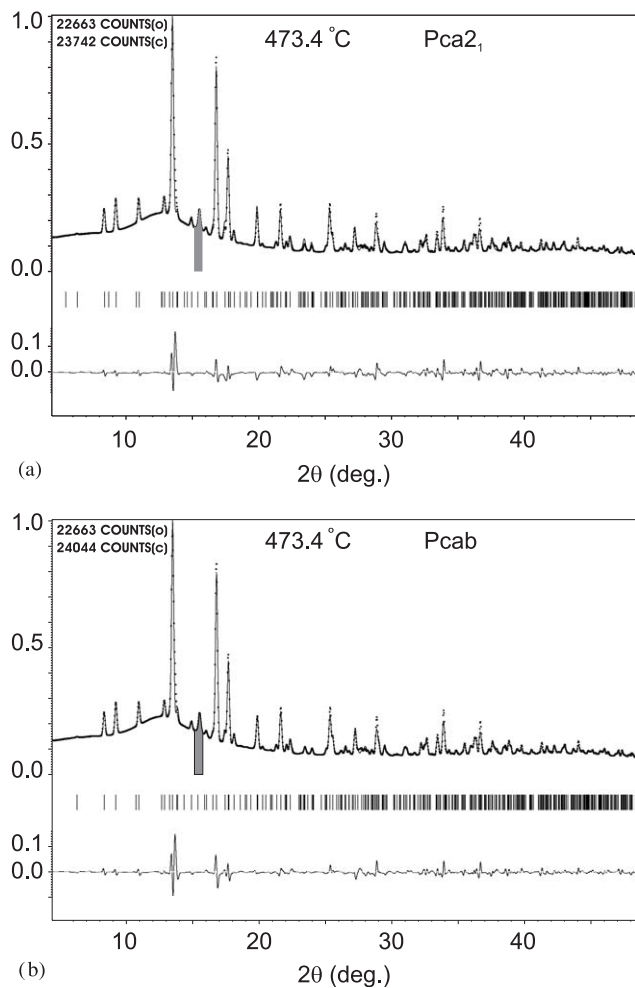


Fig. 4. Rietveld plot of the X-ray diffraction at 473.4 °C for refinement of a structure model in (a) space group *Pca*2₁; (b) space group *Pcab*. Shown are the measured and calculated intensities (upper trace), the reflection markers and the difference between observed and calculated intensities (lower trace). The shaded area contains a peak due to quartz and was excluded from the refinements.

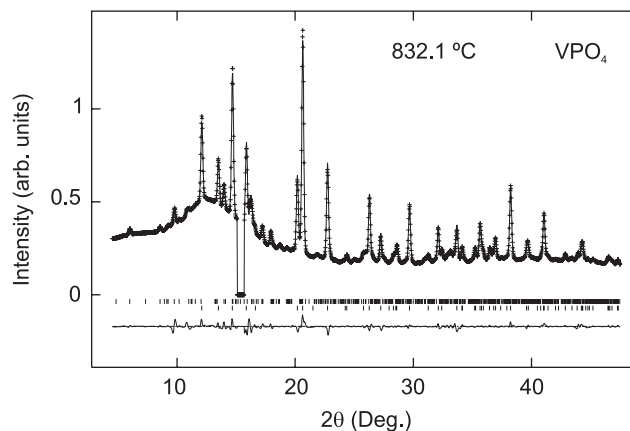


Fig. 5. Rietveld plot of the X-ray diffraction at 832.1 °C. The intense diffraction maxima are all explained by the VPO₄ structure (lower trace of reflection markers), while the remaining diffraction peaks are due to the impurity phase V₄(P₂O₇)₃.

dance with the large anisotropic expansion along **a** (Fig. 3b). The latter indicates rearrangements of the atoms within the unit cell in dependence on temperature, as opposed to a homogeneous expansion. This could be the result of rotations of the polyhedral groups, thus eventually leading to a structure of higher symmetry.

Diffraction maxima indicating a second phase were first observed in the pattern recorded at 491.3 °C. Their intensities increased on increasing temperature, up to 670.7 °C. These diffraction maxima could be indexed by a unit cell of $a_2 = 7.3669$, $b_2 = 9.6659$ and $c_2 = 21.359$ Å, indicating that this second phase is V₄(P₂O₇)₃ [25]. The second phase persisted into the high-temperature phase, but it represented a minority phase at all temperatures.

With an onset at $T = 706.5$ °C the bulk of the material transformed into a new phase, that was identified as VPO₄ [26]. The transformation was complete at $T = 796.2$ °C. The three diffraction patterns taken at 796.2, 814.1 and at the highest temperature studied, 832.1 °C, could all be very well explained by the structure of VPO₄, with V₄(P₂O₇)₃ as minority phase [25,26] (Fig. 5).

3. Discussion

3.1. Anisotropic thermal expansion

We have found that vanadyl pyrophosphate is stable up to a temperature of $T = 473.4$ °C. Below $T_c = 214.1$ °C the thermal expansion is anisotropic with a linear expansion along **a** that is almost an order of magnitude larger than that along **b** and **c**. This behavior continues the anisotropic expansion as it was observed between 100 and 295 K [27]. At 214.1 °C the

anomalously large expansion along **a** stops, and the thermal expansion becomes nearly isotropic (Fig. 3b). At this temperature the thermal expansion itself (α_V) also changes (Fig. 3a), thus suggesting a second-order phase transition to occur at $T_c = 214.1^\circ\text{C}$. A good candidate for the high-temperature form of $(\text{VO})_2\text{P}_2\text{O}_7$ is a structure with symmetry $Pcab$, that can be obtained from the low-temperature $Pca2_1$ structure by relatively small rotations of the metal oxygen polyhedra, as they are presumed to be at the origin of the anisotropic thermal expansion. This interpretation is further supported by the good fit of the $Pcab$ structure to the diffraction data (Fig. 4) and by the fact that a transition from $Pcab$ towards $Pca2_1$ is allowed to be second-order by symmetry [28].

3.2. High-temperature stability of $(\text{VO})_2\text{P}_2\text{O}_7$

With an onset at $T = 491.3^\circ\text{C}$ a second phase develops in our sample, that was identified as $\text{V}_4(\text{P}_2\text{O}_7)_3$. The gradual increase with temperature of the intensities of the Bragg reflections corresponding to this phase should not be interpreted as a shift of the equilibrium between the two phases with temperature, because it is known from several studies that the reactions of $(\text{VO})_2\text{P}_2\text{O}_7$ with, for example, oxygen are slow [4] and our experiment lasted for 2 h only. $\text{V}_4(\text{P}_2\text{O}_7)_3$ is a reduced compound as compared to $(\text{VO})_2\text{P}_2\text{O}_7$, with a valence of vanadium of $3+$. Therefore this phase cannot be the result of oxidation of $(\text{VO})_2\text{P}_2\text{O}_7$, e.g. by the tiny amount of oxygen in our capillary. Instead, it might be the result of decomposition of $(\text{VO})_2\text{P}_2\text{O}_7$ into an oxygen-rich phase $(\text{VO})_2\text{P}_2\text{O}_{7+\delta}$ with the $(\text{VO})_2\text{P}_2\text{O}_7$ -type structure and the reduced phase. This interpretation is in accordance with reports in the literature, where the presence was proposed of interstitial oxygen between the layers in the $(\text{VO})_2\text{P}_2\text{O}_7$ structure [4,29]. Also, the anomalously large thermal expansion of the **a**-axis above $T = 491.3^\circ\text{C}$ supports this interpretation. Furthermore, it is in agreement with the observation that a low but finite oxygen partial pressure is required for the stabilization of $(\text{VO})_2\text{P}_2\text{O}_7$ at high temperatures [12,30].

Between 706.5 and 796.2°C $(\text{VO})_2\text{P}_2\text{O}_7$ transforms into VPO_4 , which is again reduced as compared to $(\text{VO})_2\text{P}_2\text{O}_7$, containing V^{4+} . This finding is in accordance with our previous observations on the decomposition of $(\text{VO})_2\text{P}_2\text{O}_7$ in true inert atmospheres [17,30], while other studies have reported the stability of $(\text{VO})_2\text{P}_2\text{O}_7$ up to 750°C [31]. We do not have a good explanation for the loss of oxygen, and we can only speculate that it will have build up some high pressure inside the capillary and thus is forced out of the capillary through minor cracks.

3.3. V–P–O catalysts

Vanadyl pyrophosphate has been shown to be the major phase of V–P–O catalysts [1]. Optimal working conditions are close to 400°C , that is in the middle of the stability region of the high-temperature form of $(\text{VO})_2\text{P}_2\text{O}_7$. The preparation of the active catalyst often involves higher temperatures up to 550°C . The importance of the proposed phase transition and the observed anisotropic thermal expansion for the understanding of the catalytic mechanism is not immediately clear. However, our results on the thermal expansion give strong support for mechanisms of catalytic behavior that involve the incorporation of additional oxygen into the $(\text{VO})_2\text{P}_2\text{O}_7$ lattice. Furthermore, detailed computations like electronic band structure calculation will have to take into account the different symmetry as well as different lattice parameters of $(\text{VO})_2\text{P}_2\text{O}_7$ at the temperature of operation of catalysts. Unfortunately, our X-ray powder diffraction data are of insufficient resolution to determine accurate crystal structures.

4. Conclusions

Vanadyl pyrophosphate has been shown to exhibit highly anisotropic thermal expansion between -170°C and $T_c = 214.1^\circ\text{C}$. The high expansion along **a** stresses the importance of the role (100) surface in catalysis. A second-order phase transition is observed to occur at $T_c = 214.1^\circ\text{C}$. It is proposed to be a transition from the known $Pca2_1$ structure towards a high-temperature form of $(\text{VO})_2\text{P}_2\text{O}_7$ with space group $Pcab$. The high-temperature structure can be obtained from the room temperature structure by rotations of the metal oxygen polyhedra.

Above 491.3°C an autoredox reaction was observed resulting in a minor amount of $\text{V}_4(\text{P}_2\text{O}_7)_3$ and probably the development of an oxygen-rich vanadyl pyrophosphate phase $(\text{VO})_2\text{P}_2\text{O}_{7+x}$ ($x > 0$). This observation strongly supports any mechanisms for the catalytic activity of vanadyl pyrophosphate catalysts, that involve additional oxygen within the $(\text{VO})_2\text{P}_2\text{O}_7$ lattice. In a non-oxidizing atmosphere vanadyl pyrophosphate was found to decomposed into VPO_4 above 706.5°C .

Acknowledgments

The work at NSLS was supported under Contract DE-AC02-98CH10886 with the US Department of Energy, Division of Chemical Sciences.

References

- [1] G. Centi, Catal. Today 16 (1993) 5–26.
- [2] F. Cavani, F. Trifiro, Catal. Today 51 (1996) 561–580.
- [3] E. Bordes, P. Courtine, J. Catal. 57 (1979) 236–252.

- [4] G. Koyano, T. Okuhara, M. Misono, *J. Am. Chem. Soc.* 120 (1998) 767–774.
- [5] P.L. Gai, K. Kourtakis, *Science* 267 (1995) 661–663.
- [6] H. Bluhm, M. Havecker, E. Kleimenov, A. Knop-Gericke, A. Liskowski, R. Schlogl, D.S. Su, *Top. Catal.* 23 (2003) 99–107.
- [7] D.C. Johnston, J.W. Johnson, D.P. Goshorn, A.J. Jacobson, *Phys. Rev. B* 35 (1987) 219–222.
- [8] D.A. Tennant, S.E. Nagler, T. Barnes, A.W. Garrett, J. Riera, B.C. Sales, *Physica B* 241–243 (1998) 501–505.
- [9] H.-J. Koo, M.-H. Whangbo, *Inorg. Chem.* 39 (2000) 3599–3604.
- [10] D.C. Johnston, T. Saito, M. Azuma, M. Takano, T. Yamauchi, Y. Ueda, *Phys. Rev. B* 64 (2001) 134,403.
- [11] Y.E. Gorbunova, S.A. Linde, *Sov. Phys. Dokl.* 24 (1979) 138–140.
- [12] P.T. Nguyen, A.W. Sleight, Vanadium phosphate catalyst: ideal structure, real structure, and stability region, in: B.K. Warren, S.T. Oyama (Eds.), *Heterogeneous Hydrocarbon Oxidation*, ACS Symposium Series, vol. 638, 1996, pp. 236–248.
- [13] Z. Hiroi, M. Azuma, Y. Fujishiro, T. Saito, M. Takano, F. Izumi, T. Kamiyama, T. Ikeda, *J. Solid State Chem.* 146 (1999) 369–379.
- [14] S. Geupel, K. Pilz, S. van Smaalen, F. Bullesfeld, A. Prokofiev, W. Assmus, *Acta Crystallogr. C* 58 (2002) 9–13.
- [15] H.-J. Koo, M.-H. Whangbo, P.D. VerNooy, C.C. Torardi, W.J. Marshall, *Inorg. Chem.* 41 (2002) 4664–4672.
- [16] E. Bordes, P. Courtine, J.W. Johnson, *J. Solid State Chem.* 55 (1984) 270–279.
- [17] A.V. Prokofiev, F. Bullesfeld, W. Assmus, *Cryst. Res. Technol.* 33 (1998) 157–163.
- [18] J.B. Parise, C.L. Cahill, Y.J. Lee, *Can. Mineral.* 38 (2000) 777–800.
- [19] P.J. Chupas, M.F. Ciruolo, J.C. Hanson, C.P. Grey, *J. Am. Chem. Soc.* 123 (2001) 1694–1702.
- [20] A.P. Hammersley, S.O. Svensson, M. Hanfland, A.N. Fitch, D. Hausermann, *High Pressure Res.* 14 (1996) 235–248.
- [21] A.P. Hammersley, ESRF Internal Report ESRF98HA01T, European Synchrotron Radiation Facility, Grenoble, France, 1998.
- [22] B. Hinrichsen, R.E. Dinnebier, M. Jansen, Powder3D, An easy to use program for data reduction and graphical presentation of large numbers, Book of Abstracts of the Nineth European Powder Diffraction Conference, Prague, 2004.
- [23] A.C. Larson, R.B.V. Dreele, GSAS—General Structure Analysis System, Los Alamos National Laboratory Report LAUR 86-748, 1995.
- [24] M. Dusek, V. Petricek, M. Wunschel, R.E. Dinnebier, S. van Smaalen, *J. Appl. Crystallogr.* 34 (2001) 398–404.
- [25] K.K. Palkiona, S.I. Maksimova, N.T. Chibiskova, K. Schlesinger, G. Ladwig, *Z. Anorg. Allg. Chem.* 529 (1985) 89–96.
- [26] R. Glaum, M. Reehuis, N. Stüßer, U. Kaiser, F. Reinauer, *J. Solid State Chem.* 126 (1996) 15–21.
- [27] P. Daniels, Unpublished.
- [28] H.T. Stokes, D.M. Hatch, *Isotropy Subgroups of the 230 Crystallographic Space Groups*, World Scientific, Singapore, 1988.
- [29] M.L. Granados, J.C. Conesa, M. Fernandez-Garcia, *J. Catal.* 141 (1993) 671–687.
- [30] A.V. Prokofiev, F. Bullesfeld, W. Assmus, *Mater. Res. Bull.* 35 (2000) 1859–1868.
- [31] J.-C. Volta, *Top. Catal.* 15 (2001) 121–129.